Indian Journal of Pure & Applied Physics
Vol. 52, June 2014, pp. 374-377

Plasmon characteristics in stage-1 graphene intercalation compounds

Sidharth Acharya & Raman Sharma*

Department of Physics, Himachal Pradesh University, Shimla 171 005, India

*E-mail: sramanb@mailcity.com, AcharyaSidharth19@yahoo.in,

Received 19 September 2013; revised 10 November 2013; accepted 21 February 2014

The plasmon characteristics in stage-1 graphene intercalation compounds (GIC's) using the massless Dirac fermion (MDF) gas approximation have been reported. The superlattice model of GIC's with negligible c-axis conductivity has been considered. With the discussion of the weak and the strong c-axis coupling at graphene-intercalant hetrojunction plasmon characteristics of GIC's are predicted. A reasonable agreement has been found between our results and the experimental results of Ritsko and Rice.

Keywords: Intercalated graphene, Dielectric function, Energy loss function

1 Introduction

Graphene intercalation compounds (GIC's) are presently the objects of many investigations attributed to their high electrical conductivity and novel crystal structure[1]. Of central importance in these studies is the nature of the electron gas responsible for the electrical properties of GIC's. The massless Dirac fermion gas approximation[2-5] (MDF) as it is known for its unusual features has been proved to be much fruitful to study the electrical properties of such layered systems.

2 Theory

The superlattice model has been considered to study stage-1 GIC's in which a single graphene layer is sandwich bounded by two adjacent intercalant layers (an atomic or molecular layer e.g., $FeCl_3$, alkali atoms etc.) or vice-versa[6-8]. It is sufficient to consider the type-II superlattice exhibiting spatial separation and confinement of electrons in graphene layer and holes in intercalant layer or vice-versa.

Consistent with the experimental[9] results, a broad three-dimensional plasmon mode is predicted at 1.4 eV, whereas a high energy plasmon mode at 5.5 eV is also observed.

The dielectric function in the random-phase-approximation[6,7] has been calculted. The results are used to examine the plasmon structure of GIC's. Lindhard (RPA): In the effective mass approximation GIC's are described by the Hamiltonian[10].

$$H=\frac{\hbar^2}{2m^*}\begin{pmatrix}0 & \mathbf{k}_-^2\\ \mathbf{k}_+^2 & 0\end{pmatrix}-\frac{\hbar^2 k_0}{2m^*}\begin{pmatrix}0 & \mathbf{k}_+\\ \mathbf{k}_- & 0\end{pmatrix} \qquad \ldots(1)$$

where the first term is quadratic in $\mathbf{k}$ describing the strongly coupled $E_F\neq 0$, system of GIC's and the second term is linear in $\mathbf{k}$ describing the weakly coupled $E_F=0$, system of GIC's. $\mathbf{k}=(\mathbf{k}_x,\mathbf{k}_y)$ is the two-dimensional wave-vector measured from the degenerate point. $m^*=0.033\ m_0$ is the effective mass of the quadratic term. The light velocity of the linear term is $v_0=\hbar k_0/2m^*=10^5$m/s, with $k_0=10^8/\sqrt{3}$m^{-1}. Dielectric function for GIC's can be written as[6,7]:

$$\varepsilon^{RPA}(\mathbf{q},\omega)=1+v(\mathbf{q})S(\mathbf{q},k_z)\chi(\mathbf{q},\omega) \qquad \ldots(2)$$

where $v(\mathbf{q})=2\pi e^2/\varepsilon_o q$ is the Fourier transform of the two-dimensional Coulomb potential. The polarization function $\chi(\mathbf{q},\omega)$ is given by:

$$\chi(\mathbf{q},\omega)=\frac{g_v g_s}{S}\sum_{ss'\mathbf{k}}\frac{f_{s'\mathbf{k}}-f_{s\mathbf{k}+\mathbf{q}}}{E_{s'\mathbf{k}}-E_{s\mathbf{k}+\mathbf{q}}+\omega}\left|c^{\dagger}_{s\mathbf{k}+\mathbf{q}}c_{s'\mathbf{k}}\right|^2 \qquad \ldots(3)$$

where $g_v=g_s=2$ are the spin and the valley degeneracy and S is the sample area. $ss'=\pm 1$ are the band indices and $|c^{\dagger}_{s\mathbf{k}+\mathbf{q}}c_{s'\mathbf{k}}|^2=[1+ss'\cos(\theta_{\mathbf{k}}-\theta_{\mathbf{k}+\mathbf{q}})]/2$ are the Coulomb matrix elements. As $\mathbf{k}\rightarrow-\mathbf{k}$, the Coulomb matrix elements vanish and indicate the absence of backscattering in GIC's. This further shows that the polarization function exhibits a strong dependence on the scattering angle. As a consequence, the static polarization function $\chi(\mathbf{q})$ for $\mathbf{q}<2\mathbf{k}_F$, is a continuously decreasing function. At $\mathbf{q}=2\mathbf{k}_F$, the matrix elements vanish identically due to the absence of backscattering and the polarization function vanishes altogether (Ando *et al*[11].). In the limit $\mathbf{q}\rightarrow 0$, the structure factor[6,7] $S(\mathbf{q},k_z)=2/\mathbf{q}I_c$ for $k_z=0$ and $\mathbf{q}I_c/2$ for $k_z=\pi/I_c$

gives two plasmon bands. Near the upper edge $k_z=0$ with $E_F\neq0$, of the plasmon band $\omega_p=\sqrt{g_v g_s[\omega_p^{o}+Aq^2]}$, where $\omega^{o}_p=[4e^2E_F/I_c\varepsilon_o]^{1/2}$, and $A=3/10\times v_f^2/\omega^{o}_p$. On the other hand, near the lower edge $k_z=\pi/I_c$ with $E_F\rightarrow0$, we have $\omega_p=\sqrt{g_v g_s A'q}$, where $A'=[2e^2E_FI_c/\varepsilon_o+3/5\times v_F^2]^{1/2}$.

3 Discussion and Conclusions

The excitations of the system can be examined in terms of corresponding peaks in the dynamic structure factor:

$$S(\mathbf{q},\omega)=-\frac{1}{nv(\mathbf{q})S(\mathbf{q},k_z)}I_m\left[\frac{1}{\varepsilon(\mathbf{q},\omega)}\right] \qquad \ldots(4)$$

It is now straightforward to examine the shape of spectra by numerical calculations. Near the lower energy edge of the plasmon band energy loss factor $\mathrm{Im}[-1/\varepsilon(\mathbf{q},\omega)]$ contains a small energy denominator ~0.4 eV for a shift in the Fermi energy~0.2 eV with γ=6.64 eV Å and $k_F=1.79\times10^6\mathrm{cm}^{-1}$. These virtual intra-band transitions v→v and c→c in the vicinity of the Fermi energy $E_F\rightarrow0$, as shown by the dispersion has very small effects on the spectra due to a continuously decreasing polarization function which vanishes for $\mathbf{q}=2k_F$.

On the other hand, near the upper edge of the plasmon band the energy denominator in $\mathrm{Im}[-1/\varepsilon(\mathbf{q},\omega)]$ contains an inter-band threshold for the inter-band transitions. The gap increases with increasing degree of charge transfer. To evaluate the spectra near upper plasmon band, the inter-band threshold[9] of 1.4ev corresponding to the degree of charge transfer f=0.1, is used. In Fig. 1 a plot of $\mathrm{Im}[-1/\varepsilon(\mathbf{q},\omega)]$ versus ω at selected **q** is shown for $k_z=0$ mode. The calculation is restricted to the region ω<3.5eV with I_c=9.42 Å and ε_o=2.5. Unlike a sharp three-dimensional delta function peak, a broad three-dimensional plasmon mode around ω≈1.4 eV is found for $\mathbf{q}=0.1\text{Å}^{-4}$. The broadening is mainly due to the existence of a weak two-dimensional plasmon mode due to the individual layer planes and extending at E_F=0. As is clear from the spectra, the broadening is a flat curve on the left and a small shoulder on the right for $\mathbf{q}=0.1\ \text{Å}^{-4}$. This means that the broadening begins with the graphene layer with low carrier concentration and ends with the intercalant layer with high carrier concentration or vice-versa. Thus, broadening is essentially a feature of the layered structure of GIC's. The broadening increases with the momentum transfer and at higher values, i.e., $\mathbf{q}=0.21\ \text{Å}^{-4}$ and $\mathbf{q}=0.28\ \text{Å}^{-4}$, the peak height in spectra falls very rapidly, and almost disappears at $\mathbf{q}=0.35\ \text{Å}^{-4}$. This further indicates that the three-dimensional nature of the plasmon is prominent only for small momentum transfer. The interesting feature is the peak height which in our spectra falls as $\mathbf{q}^{-4}$ which is a characteristic of uniform three-dimensional Fermi gas.

For high incident energies, the degree of charge transfer along the c-axis increases severely. We computed[12] for the degree of charge transfer f = 1.2, a shift in the Fermi energy~2.8 eV for C_6FeCl_3. This causes an inter-band threshold of 5.6 eV, with a typical carrier density of $10^{12}\ \mathrm{cm}^{-1}$. The gap varies only negligibly with further charge transfer (f=1.2-1.6) due to the large density of states near the Fermi level. For a given Fermi energy GIC's exhibit the dispersion given by $k_z=\pi/I_c$ mode and the situation is not very different from a doped bilayer graphene[10]. The corresponding peaks are shown in Fig. 2 for $k_z=\pi/I_c$ mode. Here, calculations are restricted to the region 3.5eV<ω<7eV. We have found a broad two-dimensional plasmon mode around ω≈5.5 eV for

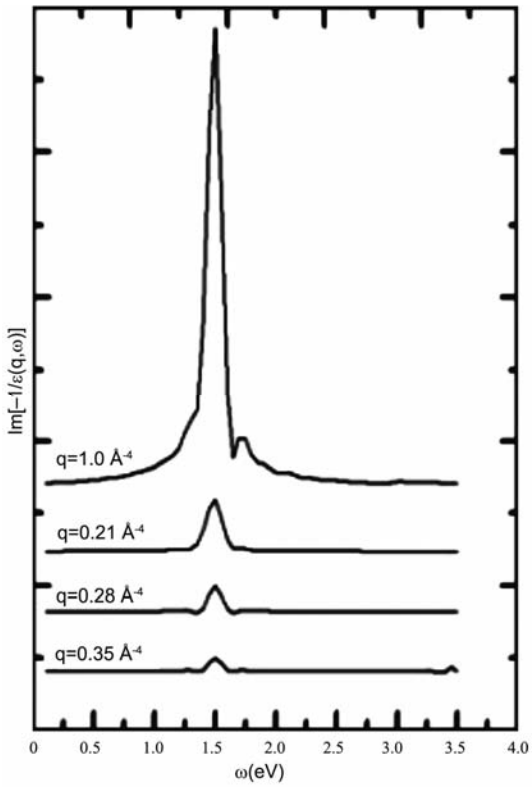

Fig. 1 — Plot of energy loss spectra of GIC's for $k_z=0$ mode at selected momentum transfer. The spectra exhibit q^{-4} dependence similar to uniform three-dimensional electron gas

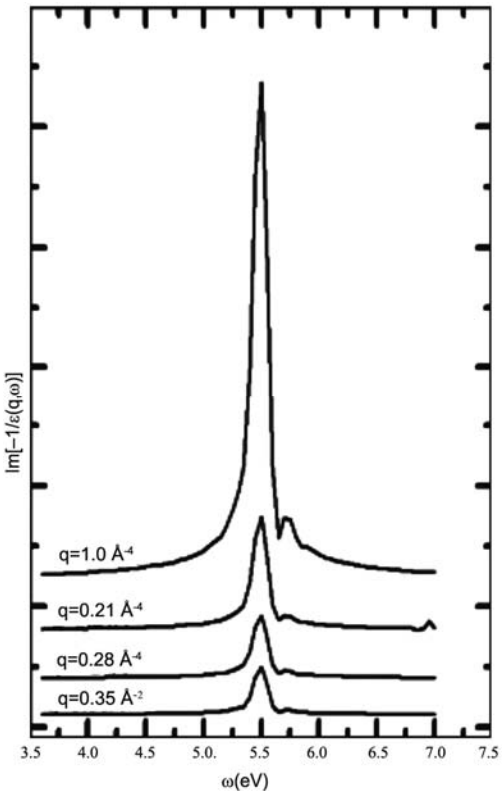

Fig. 2 — Plot of energy loss spectra of GIC's for $k_z=\pi/c$ mode at selected momentum transfer. The spectra exhibit q^{-2} dependence similar to uniform two-dimensional electron gas

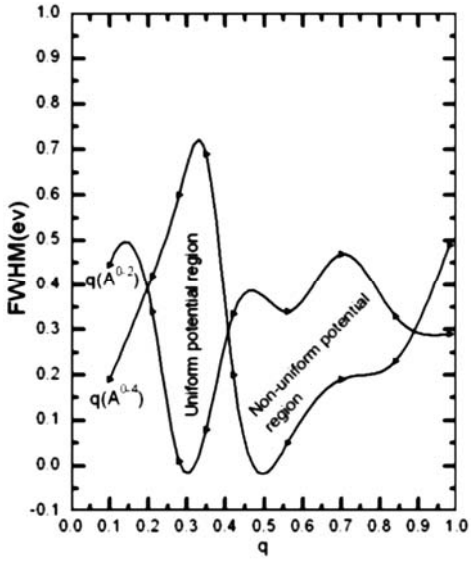

Fig. 3 — Plot of plasmon widths (FWHM) of the energy curves. This shows the nature of c-axis correlations in GIC's

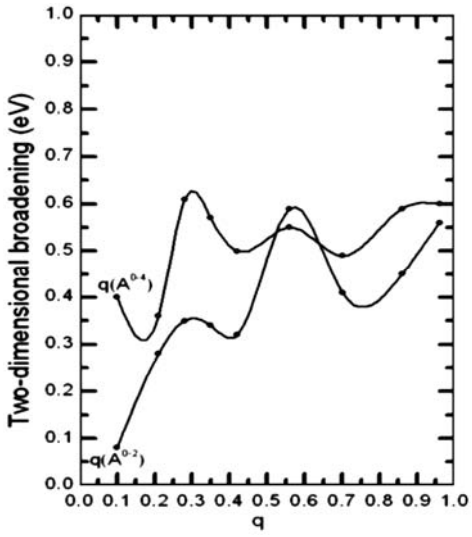

Fig. 4 — Plot of two-dimensional broadening of the energy curves

q=0.1 Å^{-2}. For higher values, i.e., **q**=0.21 Å^{-2} and **q**=0.28 Å^{-2}, the fall in the peak height is small and a number of peaks upto **q**=0.35 Å^{-2} and above can be observed in the spectra. This indicates that the broadening depends only on the carrier density of individual layer planes. Energy loss in this case can only take place in the creation of electron hole pairs at the graphene-intercalant hetrojunction which gives rise to the observed spectra. The peak height in the spectra falls as $\mathbf{q}^{-2}$, which is a characteristic of uniform two-dimensional electron gas.

In Fig. (3), we have a plot of plasmon widths, i.e., full width at half maximum (FWHM) versus **q** of the energy curves as shown in Figs 1 and 2. These measurements provide relevant information of the c-axis correlations in GIC's. For the $\mathbf{q}^{-4}$ dependence of the plasmon width the curve shows an increase in the energy resolution from 0.19eV to 0.7eV for 0.1 Å^{-4} ≤**q**≤0.35 Å^{-4}. Thereafter, the curve shows a sharp decrease in the energy resolution to 0.05 eV for **q**=0.56 Å^{-4}, which is expected due to strong **q** dependence along c-axis. Thus, the three-dimensional plasmon in GIC's has an exceptional stability for small **q**. For the higher **q** values, **q**=0.56 Å^{-4}≤**q**≤ 0.98 Å^{-4} the curve is unstable. This is attributed to the non-uniformity of the potential as the two-dimensional effects become more important. For the $\mathbf{q}^{-2}$ dependence on the other hand, the curve shows a valley of stability in the energy resolution from 0.4 eV to a sharp minimum at 0.01eV which then increases to 0.33 eV for **q**=0.1 Å^{-2}≤**q**≤0.42 Å^{-2}. For higher **q** values, i.e., 0.42 Å^{-2}≤**q**≤0.98 Å^{-2}, the curve is unstable. The valley of stability is attributed to the

energy loss that takes place in the creation of electron-hole pairs at the graphene-intercalant hetrojunction. The curve becomes unstable near the Zener breakdown which in general is characteristics of a semiconducting hetrojunction. An interesting feature which can be observed from the FWHM curves is that the two curves cut each other at three distinct points. This indicates that the π band structure is not grossly perturbed in GIC's.

In Fig. 4 we have a plot of two-dimensional broadening versus **q** of the energy curves as shown in Figs 1 and 2. This provides important information about the layered structure of GIC's. For the $\mathbf{q}^{-4}$ dependence broadening varies rapidly with **q** for 0.1 $Å^{-2} \leq \mathbf{q} \leq 0.42$ $Å^{-2}$. This is due to increase in the degree of charge transfer along the c-axis. For higher **q** values, the broadening is almost constant because of a large density of states near the Fermi level where the two-dimensional effects becomes more prominent. Broadening also exhibits a similar trend for the $\mathbf{q}^{-2}$ dependence except for the fact that the broadening energies are lowered severely because of the two-dimensional behavior of GIC's. Broadening is highly unstable in the breakdown region.

To conclude, we have used the special band structure of GIC's which in the limits of low and high energies explores the plasmon characteristics of GIC's.

Acknowledgement

The work is supported by University Grants Commission (UGC), New Delhi under UGC Fellowship in Sciences.

References

1 Dresselhaus M S & Dresselhaus G, *Adv* Phys, 30 (1981) 139.
2 McCann E & Fal'ko V I, *Phys Rev Lett*, 96 (2006) 086805, K S Novoselov & A K Geim, *ibid*, 2 (2006) 620.
3 Koshino M & Ando T, *Phys Rev B*, 73 (2006) 245403.
4 Nilsson J, Neto A H Castro, Peres N M R, & F Guinea, *Phys Rev B*, 73 (2006) 214418.
5 Ohta T, Bostwick A, Seyller T, Horn K & Rotenberg E, *Science*, 313 (2006) 951.
6 Sarma S Das & Quinn J J, *Phys Rev B*, 25 (1982) 7603.
7 Shung Kenneth W- K, *Phys Rev B*, 34 (1986) 979.
8 Lin M F, Huang C S & Chuu D S, *Phys Rev B*, 5513 (1997) 961.
9 Ritsko J & Rice M J, *Phys Rev Lett.* 42 (1979) 666.
10 Wang Xue-Feng & Chakraborty T, *Phys Rev B*, 75 (2007) 041404.
11 Ando T, *J Phys Soc Jpn*, 75 (2006) 074716.
12 Nagayoshi H, Nakao M Tsukada K & Uemura Y, *J Phys Jpn*, 35 (2006) 396.